



ELSEVIER

Comput. Methods Appl. Mech. Engrg. 191 (2001) 515–524

**Computer methods
in applied
mechanics and
engineering**

www.elsevier.com/locate/cma

Asymmetric turbulent jet flows

J.E. Akin^{a,*}, J. Bass^b

^a *Department of Mechanical Engineering and Materials Science, Rice University – MS 321, 6100 Main Street, Houston, TX 77005, USA*

^b *Altair Engineering, 7800 Shoal Creek Blvd., Austin, TX 78757, USA*

Received 25 January 2000; received in revised form 21 December 2000

Abstract

Some of the novel features of non-circular asymmetric turbulent jet flows are introduced. The computational methods employed to verify those features are outlined and details about the differences in power levels are presented. Typical applications of asymmetric nozzles to mixing and cleaning are discussed. Significant advantages over standard circular nozzles are shown in some cases. © 2001 Elsevier Science B.V. All rights reserved.

1. Introduction

Most jet flow studies and applications have been directed to axisymmetric jets for the simple historical reason that it is much easier and economical to produce them. They are so common in our culture it is easy to see why we seldom ask in if some asymmetric nozzle shape might be better for a particular application. Our analytic, computational, and experimental studies began with the question of whether a optimal nozzle geometry exists for jets being employed to clean surfaces. Most such applications utilize a high Reynold's number ($6e5 < Re < 1.5e6$) flow and are clearly turbulent. The classical analytical studies of Abramovich [1] and Rajaratnam [28] were reviewed in hopes of finding extensions to asymmetric interior and exterior flows. But it became clear that modern computational techniques were likely to be more rewarding. A review of the literature yielded a wide variety of experimental work, but few computational fluid dynamics (CFD) studies.

Several studies addressed the flow through non-circular orifices in flat plates. A few experimental studies for non-circular jets were found but they were all for jets that had a very smooth interior shape transition from the circular inlet to the non-circular outlet. See [14,15,21,24,27]. However, we were interested in more complex interior geometries leading to a relatively sharp exit edge. Typical methods for computational models of turbulent flows were reviewed. See [7,9,10,12,13,17,22,25,26,29].

Insight into jet flows can be attained from common flow visualization methods. Typical images from [30] show the laminar vortex rings for impinging circular jets. They are shed at equal time intervals and translate downstream while remaining in the same plane. They also retain their axisymmetric location in the plane of translation. Simple analytical studies of non-circular orifices and jets show a very different type of vortex “ring” motion. For example, Kambe and Takao [20] have studied non-circular vortex “rings” that start in a plane, as they would for a typical jet, and then propagate in a direction normal to the original plane. Fig. 1 shows that an originally elliptical vortex ring in a plane will attempt to take on a circular shape as it

* Corresponding author. Tel.: 713-348-4879; fax: +713-348-5423.
E-mail address: akin@rice.edu (J.E. Akin).

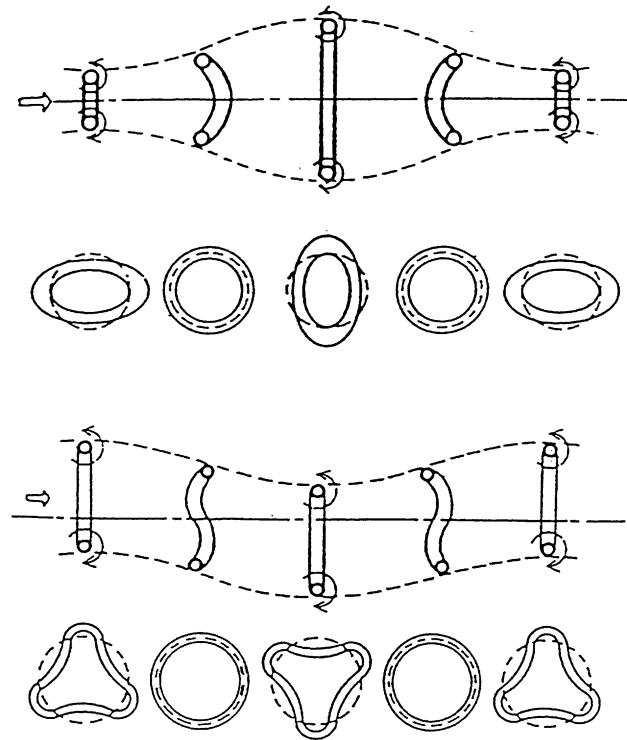


Fig. 1. Typical non-circular vortex ring distortions.

propagates downstream. However, in the process of doing so most of the vortex ring moves out of its original plane. As it continues to distort back into a planar shape it becomes elliptical again, but its major axis has rotated by 90° . Then, the process of in-plane and out-of-plane distortions repeats itself. For a three lobe planar vortex “ring” the distortions and “axis switching” becomes more complex. Experimental measurements of this phenomenon, for turbulent elliptical orifices, have been published by Ho and Gutmark [16,19]. For non-circular jet flow this vortex “ring” axes switching motion is called “vortex induction”. It is in large part responsible for a large increase in the mixing and entrainment of surrounding fluid into the jet flow. It causes large shear layers that are, of course, asymmetric and change as they move downstream. The asymmetric jets also create asymmetric and larger turbulent flows. These aspects of asymmetric turbulent jet flow make them well suited for applications involving mixing, cleaning, and combustion.

2. CFD considerations

Published CFD models of asymmetric jet flows are rare. Deshpande and Vaishnav [11] conducted laminar CFD studies of circular impinging jets. Brueckner and Pepper [8] have presented a computational study of a transonic flow through a rectangular nozzle. It involved a swirling input flow that had a noticeable effect on the vortex rings in downstream planes. However, it employed a smooth “S” shaped transition curve, in each radial plane, from the circular inlet to the rectangular outlet. That makes the internal nozzle shape different from the types that are considered here. In the applications to be modeled here the interior nozzle transition shapes are typically not smooth and the exit angles vary around the exit perimeter. By way of comparison, most jets utilize a uniform exit angle around the exit perimeter. The importance of the geometry of the asymmetric interior transition surface means that the finite element model must use a fine mesh interior to the jet and then transition to the submerged mixing domain that is semi-infinite or at least quite large compared to the nozzle outlet area. Several of the asymmetric interiors

also include sharp edges that are nearly parallel to the input axis and are designed to shed nearly axial vortices that must be captured by the internal CFD model. Thus the flows of interest are occurring at high Reynold's numbers, have high turbulence levels, significant recirculation and mixing, and large length scale differences between the flows internal and external to the nozzle. Initial attempts to apply CFD techniques to these problems involved academic CFD codes [3], and typical commercial finite element and finite volume CFD systems. These typically failed to converge and/or were very expensive and difficult to use.

These experiences led to the opinion that an adaptive solution technique would be required especially since results for parametric studies of several interior geometries were desired. The *hp*-adaptive finite element CFD approach appeared, correctly, to offer the most efficient and reliable solutions. Thus a modified kernel was developed for use with the ProPhlex CFD code [6]. That *hp*-adaptive finite element CFD system employed the full three-dimensional Navier–Stokes equations along with a $k-\epsilon$ turbulence model closure [23]. It employs automatic mesh refinement/de-refinement ability with elements having polynomial degrees ranging from one to eight. The Ainsworth–Oden error estimator [2] for the Navier–Stokes equations controlled the adaptive process. The specialized kernel was utilized mainly for auxiliary calculations to be considered later. Most of the elements in the flow domain remained at low polynomial orders with the exceptions being mainly the turbulence closure interpolations that often rise to 6th degree in the few elements located at the boundary layers. With these capabilities the lack of convergence experienced with several other approaches was no longer a problem and a large number of alternate interior geometries and external flow domains were successfully solved in a series of parametric studies of mixing and impinging flows.

3. Nozzle geometries

The asymmetric geometries of interest in this study are designed to transition from the circular inlet to an exit area that is usually offset from the inlet axis. Most of the outlet areas are non-circular in shape and all are designed to have a varying transition surface slope along the exit perimeter. The interior transition surface, of course, begins at the circular inlet and consists of primarily of two regions. The first is essentially an offset cone with a small exit radius generally located near the centroid of the outlet area. The second area is referred to as a flute. It is formed as a Boolean volume cut from the exterior volume of the offset cone. Translating a circular area along a space curve would typically form the fluted volume removed. The cut

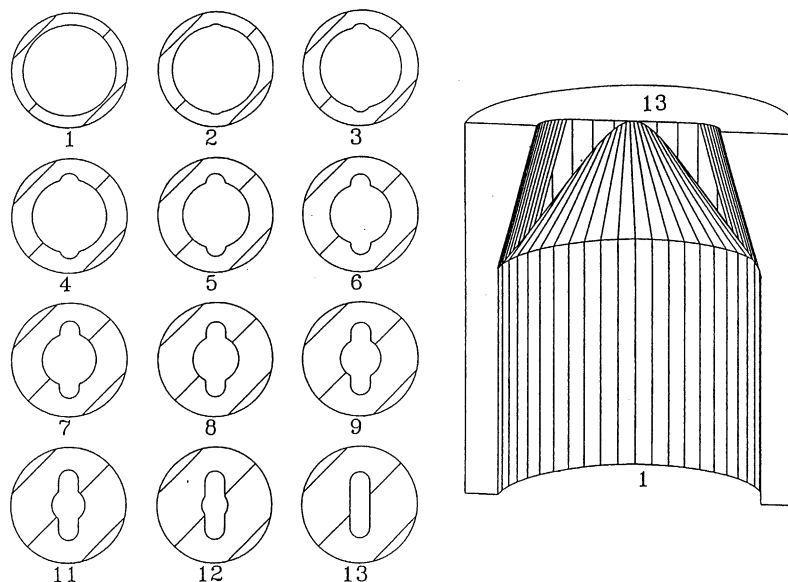


Fig. 2. A non-circular outlet fluted asymmetric nozzle.

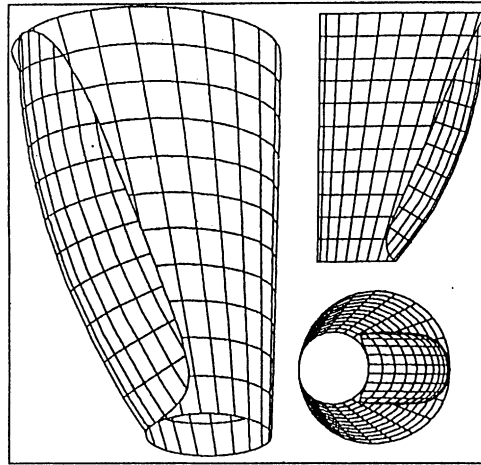


Fig. 3. Offset circular outlet “Fluted Cone” asymmetric nozzle.

reduces to zero at the inlet so that the fluid initially enters the flute tangent to the perimeter of the circular inlet of the nozzle. The flute angle, relative to the inlet axis, reaches its maximum at the perimeter of the asymmetric outlet shape.

As a result of the constructive solid geometry Boolean cut, there is a sharp edge between the offset cone surface and the flute surface. Consider a line located at the centroid of the outlet area and orientated parallel to the inlet axis. In a classical circular nozzle all of the exiting fluid velocity vectors would be parallel to this line. That is not the case in the asymmetric jets, by design. The angle between the reference line and the exiting velocity vector is maximum at the center of the flute perimeter section(s) and then decreases with increasing distance along the perimeter of the exit area. Thus, the fluid stream exiting the asymmetric jet has continuously varying and fully three-dimensional velocity vectors, instead of all being parallel. The components of the velocity normal to the reference line will be shown to be important in later discussion of the hydraulic power of the jet flow. At any planar section normal to the inlet axis the relative areas in the flute and the offset cone are varied so as to control the axial gradient of the average velocity.

Fig. 2 shows the interior transition shape for the original asymmetric nozzle in this series of parametric studies. The most recent geometry studied is shown in Fig. 3. It differs from the others in that its outlet area is circular, but offset from the inlet axis. It has flow characteristics similar to the other asymmetric geometries studied.

4. Asymmetric jet exit flows

The flow through the fluted jets is clearly fully three-dimensional. One can gain some insight into the interior nozzle flow differences by averaging the velocity over the interior cross-sectional area and comparing those averages to the classic one-dimensional circular jets for the same flow rate, inlet area, and outlet area. Of course, they must therefore have the same inlet and outlet average velocities. The fluted jet is designed, in part, to maximize the velocity gradient at the outlet. The fluid shear stresses are proportional to the axial velocity gradients, so this helps create high shear stresses at the outlet flow area of the fluted nozzles. The increased shear stresses are important in the full three-dimensional calculations of hydraulic power, but drop out of a one-dimensional approximation of the flow. Another fluid mechanics consideration is that the turbulent energy and turbulent momentum both involve the product of the velocity and its gradient. That product is usually zero at the standard nozzle outlet, but is designed to be quite large for the fluted geometry exit shapes. Thus the fluid exiting the fluted design has more turbulent energy and turbulent momentum than a classic axisymmetric nozzle. These concepts are illustrated in Fig. 4. The velocity isosurfaces for the geometry in Fig. 3 are shown in Fig. 5. By way of comparison a standard circular jet has a tight and smaller pencil-shaped set of velocity isosurfaces.

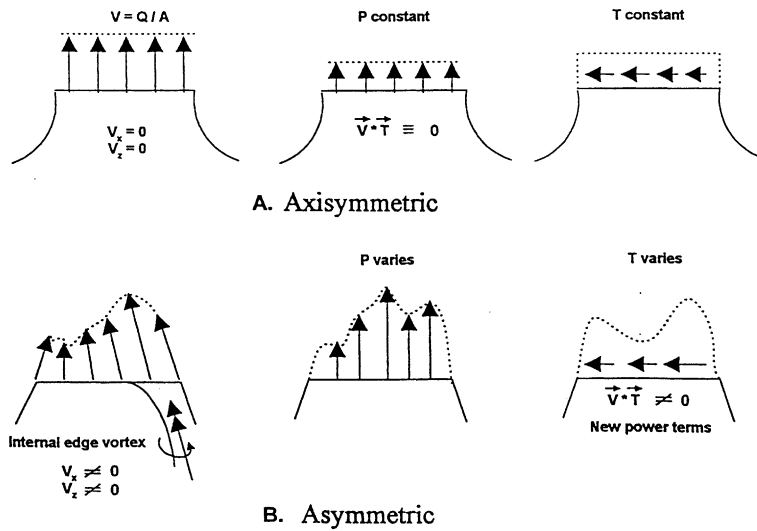


Fig. 4. Exit flow differences between asymmetric and axisymmetric jets.

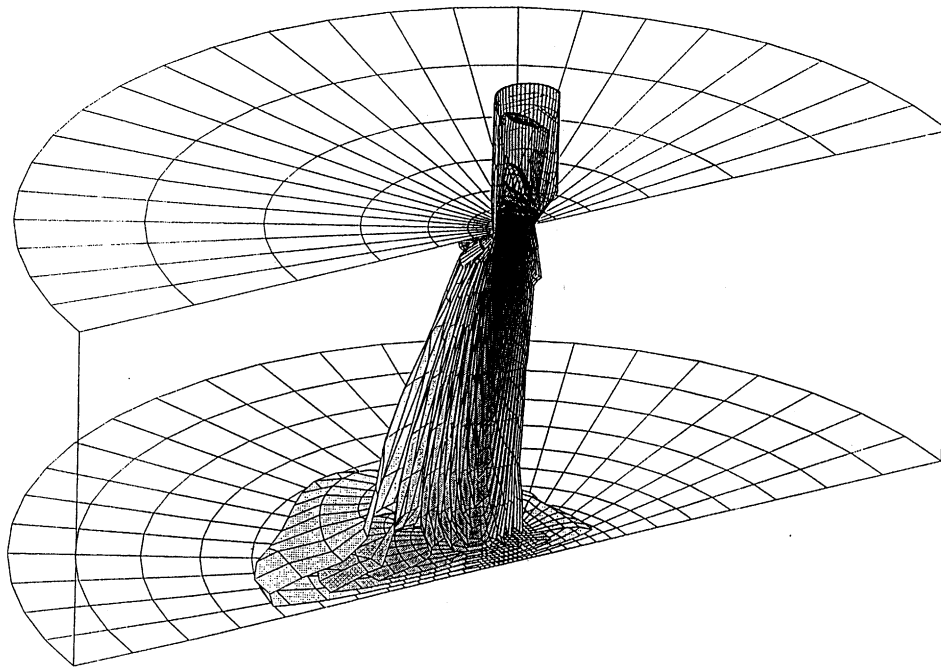


Fig. 5. Velocity isosurfaces for the “Fluted Cone”.

5. Negative impingement pressure

A novel hydraulics feature of the asymmetric fluted jets, such as those in Figs. 2 and 3, is the way the asymmetric interior transitional geometry of the jets causes suction, or less than hydrostatic, pressure to be developed on selected regions of an impingement surface. This “negative pressure” aspect of the fluted jets was demonstrated with experimental tank tests in water, and CFD studies with ProPHLEX also verified this new hydraulic phenomena [4]. Initially, it was speculated that the negative impingement pressure was the main reason that improved cleaning and mixing performance was observed when standard circular jets were replaced with the fluted jets. Fig. 6 illustrates the impingement pressure distribution for the fluted asymmetric jet shown in Fig. 3. A portion of the area develops a negative pressure that is about 20% as



Fig. 6. Impingement pressure contours for the “Fluted Cone” include regions of less than hydrostatic pressure.

large as the maximum stagnation pressure. By way of comparison, the impingement pressure contours of circular jets are concentric circles and their magnitude rapidly decreases with the radial distance. However, experimental measurements had shown that the local entrainment of re-circulating fluids increase by a factor of four or more which, in turn, may help assist in cleaning by removing particles on the impingement surface. Now, a few years later, additional studies have proved that the fluted nozzles have additional significant hydraulic behavior as a result of their three-dimensional flows.

6. Hydraulic power calculations

Early laboratory experiments with using the asymmetric jet flows in drilling and cleaning applications demonstrated a consistent and significant performance increase over standard circular nozzles of the same

size and operating at the same flow rate [5]. While the pressure drop in the asymmetric nozzle was slightly higher than for the circular jets the experimental measurements and observations implied that the asymmetric jets were imparting more power to the fluid. When thinking of the classical one-dimensional definition of hydraulic power it was not clear that a difference in power levels could be developed. However, recognizing that the fluted jet flows are fully three-dimensional it was decided to review the basic definition of hydraulic power rather than begin with one-dimensional assumptions. As shown below, starting from basic principles we find that significant differences in power levels do occur when the asymmetric jets are utilized.

Mechanical power is the scalar dot product of the velocity vector, V , at a point with the force vector at the point. The power that a nozzle imparts to the fluid flowing through it is obtained by considering the forces on the surface of its control volume. There the traction vector, f , per unit area, times the differential surface area is the needed force. The surface area of the nozzle, Γ , is made up as the union of three portions; the inlet, Γ_1 , the outlet, Γ_0 , and the wall, Γ_w . Let f_j denote the components of the traction force on the surface and V_j be the velocity vector components. Then the hydraulic horsepower, HHP, is

$$\text{HHP} = \int_{\Gamma} \vec{V} \cdot \vec{f} \, dA = \int_{\Gamma_1} \vec{V} \cdot \vec{f} \, dA + \int_{\Gamma_w} \vec{V} \cdot \vec{f} \, dA + \int_{\Gamma_0} \vec{V} \cdot \vec{f} \, dA$$

but for a viscous fluid, the velocity on the wall surface is zero, so we drop the middle term. Of course, the wall surface influences the power by influencing the spatial distribution of both the velocity, V_j and fluid stresses, τ_{ij} , and thus, the surface tractions, f_j . In the case of fluted nozzles, the wall geometry is introducing “axial” vortices and angular momentum to create components in the velocity and surface tractions, V_j and f_j that are not present in standard circular nozzles. Let σ_{ij} denote the components of the stress tensor in the fluid. Then at any surface point, recall that the surface traction force, per unit area, is

$$f_j = \sigma_{ij}n_i,$$

where the n_i are the components of surface outward unit normal vector. Thus, the nozzle power for a viscous fluid can be expressed as

$$\text{HPP} = \int_{\Gamma_1} V_j \sigma_{ij} n_i \, dA + \int_{\Gamma_0} V_j \sigma_{ij} n_i \, dA. \tag{1}$$

For the standard nozzles, the inlet and outlet normal vectors have equal components, but opposite signs. A related quantity is the volumetric flow rate, Q , which for an incompressible fluid, is

$$Q = \int_{\Gamma_1} V_j n_j \, dA = \int_{\Gamma_0} V_j n_j \, dA = \int_A \vec{V} \cdot \vec{n} \, dA, \tag{2}$$

and is usually expressed as $Q = VA$, where V is the mean one-dimensional velocity over the area A . The constitutive relations give the stress components as

$$\sigma_{ij} = -p\delta_{ij} + \tau_{ij},$$

where p is the hydrostatic pressure, τ is the viscous stress tensor, and δ is the Kronecker delta operator (identity matrix).

Now consider the axisymmetric circular nozzle based on the usual one-dimensional assumptions. Let p_1 and p_0 denote the constant inlet and outlet pressures. The velocity in, V_1 , and out, V_0 , are normal to the cross-section and parallel. Thus, only the normal traction component (pressure) is needed. The unit normal vectors are equal and opposite when the inlet and outlet areas are parallel. In that common special case the power is

$$\text{HPP} = - \int_{A_1} p_1 V_1 \cdot \vec{n}_1 \, dA - \int_{A_0} p_0 V_0 \cdot \vec{n}_0 \, dA$$

but assuming the one-dimensional pressures are constant on each area, so that their values come out of the integrals the power of the fluid exerted on the nozzle is simply

$$\text{HPP} = p_1 \int_{A_1} V_1 \cdot \vec{n}_O \, dA - p_O \int_{A_O} V_O \cdot \vec{n}_O \, dA = p_1 Q - P_O Q = (p_1 - p_O) Q.$$

Let Δp be the pressure drop across the nozzle. Then the power applied to the fluid by the nozzle is the classical expression

$$\text{HHP} = Q \Delta p \quad (3)$$

for the circular nozzle. These standard assumptions neglect terms that are present in the fluted nozzle three-dimensional flow. For example, even if the inlet pressure were constant and the inlet velocity vectors were all parallel to each other and normal to the surface, the fluted outlet velocity vectors are not parallel to each other, or the normal vector. The outlet pressure is spatially varying over the outlet area. Furthermore, the viscous stress tensor and the vorticity tensor are not zero over the outlet due to the spatial gradients of the velocity there which are induced by the interior wall geometry. It is very difficult to create analytic descriptions of these quantities for a fluted nozzle, but they are regularly computed in the CFD models. It is feasible to extend the special features of the kernel for the CFD program, such as the ProPHLEX *hp*-adaptive kernel [23], to calculate the above items for any nozzle evaluation. That is done by numerically integrating the appropriate terms over those portions of the *hp*-mesh that correspond to the nozzle inlet and outlet surfaces.

Call the CFD power calculation obtained by numerical integration over the nozzle surfaces HHP_f . We still need to relate it to the flow rate and pressure drop, Q and Δp , used in the common one-dimensional expression for hydraulic power given in Eq. (3). For any CFD run, Q is known and the pressure at any point is computed. We employ a power correction coefficient, C_f , for the fluted nozzle such that

$$\text{HHP}_f = C_f Q \Delta p = Q \Delta p_{\text{ave}}, \quad C_f = \text{HHP}_f / Q \Delta p_{\text{ave}}, \quad (4)$$

where the average pressure drop is obtained from the modified CFD kernel as

$$\Delta p_{\text{ave}} = \frac{1}{A_O} \int_{A_O} p_O \, dA - \frac{1}{A_1} \int_{A_1} p_1 \, dA. \quad (5)$$

The viscous shear contribution, that is missing in the power calculation for a circular nozzle, is defined for a Newtonian fluid as

$$\tau_{ij} = \mu(u_{i,j} + u_{j,i})$$

and thus in general the hydraulic power from the nozzle for a viscous fluid is

$$\text{HPP} = \int_{\Gamma} u_j (-p \delta_{ij} + \mu(u_{i,j} + u_{j,i})) n_i \, dA.$$

Similar analytic forms are available to describe non-Newtonian fluids. While all of these terms are active in the three-dimensional fluted nozzle flows it is easy to see that most of these terms drop out of the power calculation when the usual one-dimensional assumptions are made. Since the stress, τ , is a symmetric tensor, there are only six of the nine terms that need to be considered in detail. Let the axial, radial, and circumferential direction in an axisymmetric nozzle be denoted as, (z, r, θ) , respectively, as i or j ranges over 1, 2, 3. The six terms, in the lower triangle of the velocity gradient tensor, are

$$2 \frac{\partial u_r}{\partial r}, \quad \left(\frac{1}{r} \frac{\partial u_r}{\partial \theta} + \frac{\partial u_\theta}{\partial r} - \frac{u_\theta}{r} \right), \quad \left(\frac{1}{r} \frac{\partial u_\theta}{\partial \theta} + \frac{u_r}{r} \right), \quad \left(\frac{\partial u_r}{\partial z} + \frac{\partial u_z}{\partial r} \right), \quad \left(\frac{1}{r} \frac{\partial u_z}{\partial \theta} + \frac{\partial u_\theta}{\partial z} \right), \quad 2 \left(\frac{\partial u_z}{\partial z} \right).$$

For a circular nozzle, $u_\theta = 0$, $\partial(\cdot)/\partial\theta = 0$, and $u_r = 0$, so that this general form reduces to

$$\begin{array}{cc} 0 & \\ 0 & 0 \\ \frac{\partial u_z}{\partial r} & 0 \quad 2 \frac{\partial u_z}{\partial z} \end{array}$$

Most circular nozzles terminate with a straight section, so there we have $\partial u_z / \partial z = 0$. Thus, of the original 11 contributions only one remains in the circular nozzle, $\partial u_z / \partial r$, which is the radial variation of the axial velocity. If we assumed a one-dimensional plug flow so that u_z is constant, then the last term would also vanish. These observations confirm that the full three-dimensional nozzle power calculations indeed reduce to the common expression, $\text{HHP} = Q\Delta p$, for circular nozzles because the shear stress contributions drop out in the latter case.

To accurately calculate all of the above integrals one must first carry out an accurate CFD analysis of the fluted nozzle. To accomplish this we employ a special kernel version of a general three-dimensional *hp*-adaptive (mesh and polynomial adaptive) finite element [2] solution of the turbulent Navier–Stokes equations [23]. While most systems employ linear polynomials, this system uses the range of linear to eighth-order polynomials necessary for maximum accuracy and efficiency. That result provides the spatially varying velocity vector, stress tensor, and turbulent contributions to the viscosity everywhere. They are in turn numerically integrated in the usual fashion [3] to yield the equations used to get the hydraulic power and fluted nozzle correction coefficients given above.

The net power for a standard jet is simply the pressure drop through the nozzle times the flow rate, Q . For a fluted jet with the same flow rate and pressure drop a higher hydraulic horsepower, HHP_f , is created in part by the inclined velocity vectors combining with the increased shear stresses. Certain drilling and cleaning hydraulics operations have recommended hydraulic power levels. Thus it is desirable to have correction coefficients available for the fluted nozzles that allow operators to compute the power from the expected flow rate and pressure drop. The larger fluted jet power value can be obtained by multiplying the classical definition of hydraulic power by the coefficient, C_f , that accounts for the three-dimensional nature of its outlet flows. Typical values of C_f for fluted jets used in drilling and cleaning applications vary with nozzle size and interior geometry. For the current design shown in Fig. 3 the correction factor has been found to range from about 1.8 in small sizes (7/32 OD) to about 2.1 in large sizes (16/32 OD).

For fluted nozzles the net power imparted to the fluid is higher because the outlet flow is three-dimensional. That three-dimensional flow causes two velocity components tangent to the outlet cross-sectional area and thus in the directions of the two shear stress components also lying in that plane. The angular momentum due to the interior edges causes the new velocity components perpendicular to the plane of Fig. 4 and the shear stress magnitudes are higher due to the high exit velocity gradients. This means that the shear stresses add significant power to the fluid in the fluted jets, but do not do so in standard jets. While the fluted jet outlet power cannot be obtained exactly in closed form because of the geometry and the turbulent nature of its flow the result can be calculated by at least two completely independent methods. The most accurate value for the flute correction term for a specific fluted geometry is obtained by using a CFD calculation for the outlet flow quantities and then numerically integrating those quantities over the outlet area to obtain the outlet power. Those calculations yielded the range of correction coefficient cited above for fluted nozzles and gave a value of unit for standard circular jets, as expected.

An independent estimate of C_f has been given by Huang [18] where the analogy between turbulent fluid flow and non-linear electrical power systems was used to bound the coefficient. Huang shows that in general the range is $2 < C_f < 3$. This agrees with various CFD results before corrections necessary to cause the same pressure drop were applied to give $1.8 < C_f < 2.1$ cited above. Therefore, it has been verified that the fluted jets will typically double the hydraulic horsepower imparted to the fluid, and thus it doubles the hydraulic horsepower per square inch (HSI), computed from the area of the impingement surface, which is a commonly used parameter in cleaning applications.

7. Conclusions

The asymmetric turbulent jet flows are challenging problems to solve even with modern CFD techniques. However, they offer significant advantages in cleaning, mixing, and drilling applications. They also offer potential benefits in other applications such as combustion. They are clearly geometry dependent and our series of parametric CFD studies are still in progress in hopes of finding even more useful transition geometries. The utilization of a *hp*-adaptive finite element computational flow model has consistently allowed

the solution to converge for high Reynold's number flows. Other finite volume and finite element systems with only linear elements usually failed to converge for the same problems.

References

- [1] G.N. Abramovich, *Theory of Turbulent Jets*, MIT Press, Cambridge, MA, 1963.
- [2] M. Ainsworth, J.T. Oden, A posterior error estimation in finite element analysis, *Comput. Methods Appl. Mech. Engrg.* 142 (1–2) (1997) 1–88.
- [3] J.E. Akin, *Finite Elements for Analysis and Design*, Academic Press, London, 1994.
- [4] J.E. Akin, S.K. Smith, N.R. Dove, Negative impingement pressure nozzle, in: G. Yagawa (Ed.), *Computational Mechanics 95*, Springer, Tokyo, 1995, pp. 1108–1113.
- [5] J.E. Akin, N.R. Dove, S.K. Smith, L.M. Smith, Asymmetric nozzle hydraulics improve bit performance, *Oil Gas J.* 97 (19) (1999) 59–64.
- [6] J. Bass, *ProPHLEX User's Manual*, Computational Mechanics Co. Inc., Austin, 1990.
- [7] P. Bradshaw, T. Cebeci, J.H. Whitelaw, *Engineering Calculation Methods for Turbulent Flow*, Academic Press, London, 1981.
- [8] F.P. Brueckner, D.W. Pepper, Parallel finite element algorithm for three-dimensional inviscid and viscous flow, *Thermophys. Heat Transfer* 9 (1995) 240–246.
- [9] A.J. Chorin, Numerical solution of the Navier–Stokes equations, *Math. Comput.* 22 (1968) 745–762.
- [10] T.J. Craft, L.J.W. Graham, B.E. Launder, Impinging jet studies for turbulence model assessment, *Int. J. Heat Mass Transfer* 36 (10) (1993) 2685–2697.
- [11] M.D. Deshpande, R.N. Vaishnav, Wall stress distribution due to jet impingement, *J. Engrg. Mech.* 109 (2) (1983) 479–493.
- [12] J.H. Ferziger, Simulation of incompressible turbulent flows, *J. Comput. Phys.* 69 (1) (1987) 1–48.
- [13] J.I. Finnie, R.W. Jeppson, Solving turbulent flows using finite elements, *J. Hydraulic Engrg.* 117 (1) (1991) 1513–1521.
- [14] S. Fujita, H. Osaka, Effect of aspect ratios on potential core length for cruciform jet, *Exp. Thermal Fluid Sci.* 5 (1992) 332–337.
- [15] E. Gutmark, K.C. Schadow, Flow characteristics of orifice and tapered jets, *Phys. Fluids* 30 (11) (1987) 3448–3454.
- [16] E. Gutmark, K.C. Schadow, T.P. Parr, D.M. Parr, K.J. Wilson, Combustion enhancement by axial vortices, *J. Propulsion* 5 (5) (1989) 555–560.
- [17] V. Haroutunian, M.S. Engelman, On modeling wall-bound turbulent flows using specialized near wall finite elements and the standard $k-\epsilon$ turbulence model, *Advances in Numerical Simulation of Turbulent Flows*, FED, vol. 117, ASME, New York, 1991.
- [18] H.I. Huang, Private communication, 1998.
- [19] C.M. Ho, E. Gutmark, Vortex induction and mass entrainment in a small aspect ratio elliptic jet, *J. Fluid Mech.* 179 (1987) 383–405.
- [20] T. Kambe, T. Takao, Motion of distorted vortex rings, *J. Physical Soc. Jpn.* 31 (2) (1971) 37–45.
- [21] S. Koshigoe, E. Gutmark, K.C. Schadow, Initial development of noncircular jets leading to axis switching, *AIAA J.* 27 (4) (1989) 411–419.
- [22] B.E. Launder, D.B. Spalding, The numerical computation of turbulent flows, *Comput. Methods Appl. Mech. Engrg.* 3 (1974) 269–289.
- [23] T.J. Liszka, W.W. Tworzydlo, J.M. Bass, S.K. Sharma, T.A. Westermann, B.B. Yavari, Pro_PHLEX – An hp -adaptive finite element kernel for solving coupled systems of partial differentials equations in computational mechanics, *Comput. Methods Appl. Mech. Engrg.* 150 (1997) 261–271.
- [24] G.F. Marsters, J. Fotheringham, The influence of aspect ratio on incompressible turbulent flows from rectangular slots, *Aeronaut. Quart.* 31 (1980) 285–305.
- [25] M.J. Morris, B.F. Carrol (Eds.), *Forum on Turbulent Flows*, FED, vol. 155, ASME, New York, 1993.
- [26] M. Nallasamy, Turbulence models and their applications to the prediction of internal flows: a review, *Comput. Fluids* 15 (2) (1987) 151–194.
- [27] W.R. Quinn, On mixing in an elliptic turbulent free jet, *Phys. Fluids A* 1 (10) (1989) 1716–1722.
- [28] N. Rajaratnam, *Turbulent Jets*, Elsevier, Amsterdam, 1976.
- [29] C. Taylor, K. Morgan, *Computational Techniques in Transient and Turbulent Flow*, Pineridge Press, Swansea, 1981.
- [30] M. Van Dyke, *An Album of Fluid Motion*, Parabolic Press, Stanford, 1990.